Advanced Powder Technology 32 (2021) 1521–1531

Contents lists available at ScienceDirect

Advanced Powder Technology

journal homepage: www.elsevier.com/locate/apt

Original Research Paper

Investigating the effects of feeding properties on rock breakage by jaw crusher using response surface method and gene expression programming

Ekin Köken [a,*], Abiodun Ismail Lawal [b]

[a] Abdullah Gul University, Nanotechnology Engineering Department, 38170 Kayseri, Turkey
[b] Federal University of Technology, Department of Mining Engineering, PMB 704, Akure, Nigeria

ARTICLE INFO

Article history:
Received 19 December 2020
Received in revised form 19 February 2021
Accepted 3 March 2021
Available online 2 April 2021

Keywords:
Jaw crusher
Crushed stone
Rock comminution
Response surface methodology
Gene expression programming

ABSTRACT

The present study investigates the effects of feeding properties on rock comminution by a laboratory-scale jaw crusher. For this purpose, detailed crushability tests were carried out on four different rock types to assess their degree of rock crushability (DRC). Various feeding sizes (9.5 – 19 mm) and quantities (500 – 1500 g) were adopted to reveal the choke feeding intensity during crushing actions. The efficiency of feeding properties was investigated through the response surface methodology (RSM). The RSM results demonstrated that the characterized feeding size (F_{80}, mm) dominates the general size reduction, whereas the feeding quantity (m_f, g) is associated with the crushing energy consumption and product flakiness. Therefore, the choke feeding intensity has a direct relation to the m_f and F_{80}. In addition, novel gene expression programming (GEP) models were employed to generate empirical formulations to predict the DRC parameters. The established GEP models have a satisfactory estimation capability. Therefore, the DRC of the investigated rocks can be optimized through the proposed GEP models based on the coupling variables of m_f and F_{80}.

1. Introduction

Rock crushing is the first mechanical comminution process after drilling and blasting operations in rock fragmentation. The energy required for comminution depends on the physicomechanical properties of the rocks and the quantity of materials being crushed [1]. Although the use of different crushers should be placed in a definite order, the efficiency of crushers may be improved, depending upon their inherent mechanism. By comparison with jaw and gyratory crushers, impact crushers, for instance, can achieve a higher production yield. However, their use is limited due to high wear rates and is thus restricted to medium or weak rocks [2].

The use of unsuitable crushers, discontinuous crushing operations, and poor-quality crushing equipment results in many difficulties that decrease product quality [3]. Therefore, researchers have sought rational solutions to improve rock aggregate production efficiency from different perspectives. Specifically, rock aggregate production was handled considering rock breakage mechanisms, improvements in product size and shape, supportive equipment, and performance of crushers [4–9]. For instance, primary crushing is performed in mines and quarry sites, and initially crushed materials are conveyed to stationary plants for secondary and tertiary crushing. This technique has been mainly embraced in Europe and has lowered the rock aggregate production cost [10].

As an alternative to the conventional crushing–screening plants, the in-pit crushing and conveying system (IPCC) has been widely adopted and utilized worldwide for open-pit mining operations [11,12]. In this context, mobile crushing units are of prime importance in sand-gravel and rock aggregate production. They are mainly endowed with gyratory, twin roll, and jaw crushers that work in harmony with various belt conveying systems [13].

Achieving the optimum outputs from rock crushing operations depends upon detailed investigations on the rock – crusher interactions (RCI). The RCI plays a crucial role in rock breakage success, where the crushing degree depends on the combinations of several factors, such as crusher performance, feeding method, and rock properties. All these parameters constitute a strong basis for sustainable rock crushing. Keeping in mind that the capacity of crushers decreases as the crushing rate increases.

At the same time, energy consumption increases in parallel with the crushing rate. Therefore, when the rock properties are

* Corresponding author.
E-mail address: ekin.koken@agu.edu.tr (E. Köken).

https://doi.org/10.1016/j.apt.2021.03.007

fixed, the crushing process should be optimized, considering operational features. Specific to jaw and cone crushers, the main parameter to optimize crushing operations is the aperture of discharge in the crushing medium. It is also known as the closed-side setting (CSS) that controls the degree of rock crushability (DRC) for compressive crushers [1,14–16]. In addition to the CSS, Johansson et al. [17] introduced a model for the evaluation of jaw crusher capacity and power draw in connection with various jaw speeds.

The other optimization tool is based on the discrete element method (DEM). The DEM provides supportive data for optimization studies. In the DEM models, feed gradation, operational features, and crusher components are mainly regarded. Recently, Barrios et al. [18] performed such DEM modeling that simulates the performance of a laboratory-scale jaw crusher. They concluded that the performance factors such as throughput, product achievement, compressive forces acting on jaw plates, size reduction ratio (SRR), and specific energy consumption could be estimated, focusing on the CSS. The specific energy consumption was also investigated through statistical and machine learning methods [19]. As a general consideration, particle size distribution (PSD) of feed, crusher setting, and speed impinge on the efficiency of an industrial jaw crusher [20]. Of the crusher settings, the CSS adjustment may be a challenging issue and necessitate standard controls. It may also be time-consuming in practical applications. Under this circumstance, the feeding rate and size fractions can be regarded as reasonable alternatives for optimal crushing operations.

As for the fundamental rock comminution issues on jaw and cone crushers, Tavares and Da Silveria [21] reported that cone crusher capacity increases with decreasing the abrasion resistance of rocks. Refahi et al. [22] found remarkable relationships between shape parameters of the feed and production yield. Olaleye [23] figured out that the rock strength directly relates to the wear and energy consumption in jaw crushers. Lee and Evertsson [24] investigated the variations in PSD of feed, which control the product achievement for specific size fractions in cone crushing. Korman et al. [25] stated that the uniaxial compressive strength (UCS) of rocks is a dominating factor for crushing energy consumption in jaw crushers. Kahraman et al. [26] and Comakli and Cayirli [27] attempted to quantify the DRC from a crushability index (CI, %) that was based on the sieve analysis of crushed particles. Köken and Özarslan [28] also proposed a size-related methodology to quantify the DRC.

It has been acknowledged that the UCS is a function of DRC regarding jaw crushers [25–28]. In contrast, the Brazilian tensile strength (BTS), Shore hardness (SH), and Los Angeles abrasion loss (LAA) were turned out to be highly correlative parameters for the evaluation of DRC in cone crushing [29]. Apart from strength properties, Köken [30] conducted size-related crushability tests using a laboratory-scale cone crusher. The study concluded that the PSD of feed controls the choke feeding intensity when the feed quantity is fixed.

The studies mentioned above have provided adequate knowledge on rock crushability as a critical phenomenon in rock aggregate science and technology. However, the existing studies by the researchers have mainly focused on three parameters for evaluating the DRC with respect to jaw and cone crushers. These are rock strength, operational features (e.g., CSS and crusher speed), and the PSD of feed. However, no quantitative data has been documented on the combined effects of feeding properties (i.e., feeding size and quantity) on the DRC for compressive crushers.

For typical crushing screening plants, jaw crushers are considered the center for optimization and modeling efforts. Optimization studies are performed to explain how energy is used during the crushing process and how it can be improved [31]. Such efforts have also been made within the industrial scale to improve the DRC with an optimal generation of fines. Based on the previous studies, it seems logical to suppose that the DRC should be investigated in more detail, considering the size and shape properties of materials fed to the crushers.

Assuming that an industrial jaw crusher operates under uncontrolled feeding conditions, the DRC for that case can be variable from the points of size reduction, energy consumption, and generation of fines when initial scalping is included. Theoretically, if the choke feeding intensity is relatively low, the throughput may not be sufficient for initial rock breakage. Otherwise, excessive specific energy consumption and wear are expected undoubtedly. In addition to those, squeezing problems are also observed in the crushing medium under extreme loading conditions. In either case, initial rock comminution cannot be performed in optimal conditions. Because of that reason, the choke feeding intensity undertakes the role of crushing efficiency. Since there is no standard approach for the evaluation of choke feeding intensity for industrial jaw crushers (Fig. 1), it is required to figure out the mechanism of choke feeding as a function of feeding size and quantity.

In this direction, the present study explores the DRC variations due to varying feeding properties using a laboratory scale jaw crusher. For this purpose, detailed crushability tests were performed on four different rock types. In the crushability tests, different feeding sizes and quantities were adopted to reveal the variability of DRC parameters. As a result of laboratory studies, these effects were discussed through several statistical and machine learning methods.

2. Materials and methods

Sampling locations and descriptive codes of the investigated rocks are listed in Table 1. Laboratory studies were divided into three parts. In the first part, mineralogical characterization of the rocks was carried out by X-ray diffraction (XRD) analyses, where a Bruker Discover D8 diffractometer was used. In the second part, phsyico-mechanical and aggregate properties were determined. For the last part, detailed crushability tests were carried out by attempting various feeding features.

The experimental flow chart for the crushability tests is given in Fig. 2. Three different feeding size fractions (S1 – S3) and feeding quantities (F1 – F3) were adopted in the crushability tests. Throughout the text, the feeding quantity and characterized feeding size were denoted conceptionally as the m_f and F_{80}, respectively. The effects of aggregate flakiness on the DRC parameters were reduced by removing or minimizing flaky particles from the feed. For this purpose, an 8 mm bar sieve was used (Fig. 2). The particles passing through the 8 mm bar sieve were removed from the feed, and the remaining were weighed based on the predefined feeding quantity (F1 – F3). The CSS of the crusher was set to 8 mm for the crushability tests. The control and calibration of the CSS were conducted after every five test cycles.

Since the amount of applied energy determines the DRC [32], the power consumption during each crushability test was measured using a high precision powermeter. The technical properties of the devices used in the crushability tests are listed in Table 2.

The current (I, A) drawn by the crusher was measured by recording them displayed on the powermeter per 0.5 s. The total current drawn by the crusher was calculated by the following equations.

$$\int_a^b f(x)dx \simeq \frac{\Delta x}{2}(f(x_0) + 2[f(x_1 + x_2 + \ldots x_{n-1})] + f(x_n)) \quad (1)$$

$$\Delta x = \frac{\Delta t}{n} \quad (2)$$

Fig. 1. Illustration of choke feeding intensity for an industrial jaw crusher a) Fully loaded feeding bunker b) Uncontrolled choke feeding intensity in the crushing chamber.

Table 1
Sampling locations and descriptive codes of the investigated rocks.

Rock type	Location	Code	Additional information
Basalt	Çaycuma – Zonguldak	R1	Concrete aggregate and paving mixture resource in northwestern Turkey
Limestone	Havran – Balıkesir	R2	Concrete aggregate and paving mixture resource in western Turkey
Limestone	Gölbaşı – Ankara	R3	Lightweight concrete aggregate resource in central Turkey
Dolomitic limestone	Yahyalı – Kayseri	R4	Paving mixture resource in central Turkey

where Δt represents the crushing time from start to finish, n is the stepsize depending upon Δt. For the sake of clarity, the Δx was assumed to be the response time of the powermeter (Δx = 0.5).

In this regard, the total energy consumption E_t (kJ) was determined by the following equation:

$$E_t = \frac{V \times \cos\phi}{10^3} \sum_{i=0}^{t} I_i \times t_i \quad (3)$$

where I is the current drawn by the crusher (A), V is the voltage (V), cos(ϕ) is the power factor of the engine propelling the crusher, and t is the crushing time (s).

The DRC was assessed based on four quantitative and one qualitative parameter. The quantitative parameters were the size reduction ratio (SRR), size distribution width (Δw), product flakiness index (FI_p), and E_t (Eqs (1)–(3)). The SRR was determined using sieve analysis results (Eq (4)).

The other size-related parameter is the Δw (Eq (5)), proposed by Evertsson [33]. In practice, similar to the SRR, the Δw is a dimensionless parameter, where higher values of Δw point out a higher rate of size reduction.

$$SRR = \frac{F_{80}}{P_{80}} \quad (4)$$

where F_{80} and P_{80} denote the theoretical square mesh aperture sizes (mm) corresponding to 80% of cumulative undersize of feed's and product's PSDs, respectively.

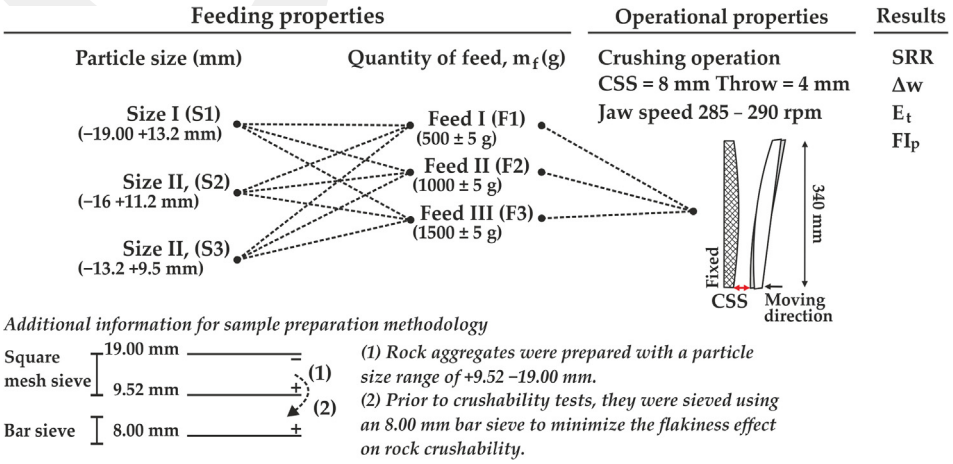

Fig. 2. Experimental flow chart for the crushability tests.

Table 2
Technical properties of the devices used in crushability tests.

Powermeter		Jaw crusher	
Nominal voltage, (V)	100 – 260	Nominal voltage (V)	220
Nominal current (A)	≤ 16	Nominal current (A)	≤ 14
Frequency (Hz)	50	Frequency (Hz)	50
Power measurement (kW)	≤ 3.68	cos(ϕ)	0.94
Response time (s)	0.5	Power (kW)	2.20
		Feeding gape (mm)	100
		Capacity (t/h)	≤ 0.2
		CSS adjustment (mm)	≤ 40
		Plate type	Convex with stiffeners
		Plate length (mm)	340
		Jaw speed (rpm)	285 – 290

$$\Delta w = \frac{P_{80} - P_{20}}{P_{50}} \quad (5)$$

where P_{80}, P_{50}, and P_{20} are the theoretical square mesh aperture sizes (mm) that correspond to 80%, 50%, and 20% of cumulative undersize of product's PSD, respectively.

The FI_p was determined by flakiness index tests conducted in accordance with BS EN 933–3 [34]. The FI_p was calculated, adopting two particle size ranges: –9.50 + 6.30 mm (FIp_1) and –6.30 + 4.75 mm (FIp_2). For the determination of FIp_1, 4 mm and 5 mm bar sieves were used together, and flaky materials passing through these sieves were averaged. On the other hand, a 3.15 mm bar sieve was used to calculate the FIp_2. The qualitative parameter to assess the DRC was based on observing failure patterns of crushed particles for different size fractions. These failure patterns were visualized by scanning electron microscope (SEM) analyses.

3. Laboratory studies

3.1. Mineralogical and failure characterization of the rocks

The mineralogical characterization of the rocks was conducted through XRD analyses, where the patterns were analyzed using the Panalytical Highscore Plus software with a mineral database of PDF[2]. Typical XRD patterns are illustrated in Fig. 3.

Based on the XRD analyses, the investigated rocks were identified as regards their lithology. Hence, the investigated rocks were found to be basalt (R1), limestone (R2, R3), and dolomitic limestone (R4). The basalts were mainly made up of four mineral groups such as plagioclase (64%), pyroxene (15%), hornblende (6), and opaque minerals (3%).

The accessory minerals were quartz (1%), clay minerals (1%), and zeolite (1%). Uncrystallized components in the basalts were defined as the matrix that constituted approximately 9% in the semiquantitative XRD analyses.

The rock types of R2 and R3 were almost composed of calcite minerals. The R4 was a dolomitic limestone with a calcite/dolomite ratio of 10 – 12. The SEM analysis demonstrated that the failure mechanisms of the rocks are quite different. For instance, fracture patterns of R1 were mainly observed as conchoidal fracture surfaces (Fig. 3a), which are typical for basaltic rocks. Because of the brittle failure, micro-fissures were evident, resulting in a splitting failure for R2 (Fig. 3b). Tabular failure is typical for R3 (Fig. 3c). Finally, intense longitudinal micro-fissures parallel to the loading direction were observed in R4 (Fig. 3d). Consequently, the failure characteristics can provide a rapid estimation of how the rocks behave under dynamic compressive forces.

3.2. Physicomechanical and aggregate properties of the rocks

The physical and mechanical rock properties were determined using core samples with a length-to-diameter ratio of 2.0–3.0. The physical properties comprised the dry unit weight (γ_d) and water absorption by weight (w_a). In contrast, the mechanical and aggregate properties considered in this study were the UCS and LAA, respectively.

The physical and mechanical properties were determined under oven-dried conditions in accordance with the methods suggested by the International Society of Rock Mechanics [35]. Nevertheless, the LAA was determined, according to BS EN 1097–2 [36]. Each test was repeated five times, and the average values were presented. The rock properties are given in Table 3. Considering the UCS values, the investigated rocks were identified from moderately hard rock (UCS = 50 – 100 MPa) to hard rock (UCS = 100 – 200 MPa), according to Deere and Miller [37].

3.3. Crushability tests

Crushability tests provide quantitative data on sizing, production yield, and comminution rate for several crushers [30]. In the context of crushability tests, rock aggregates with a particle size range of 9.52 – 19 mm were prepared (Fig. 4a). As mentioned previously, the flaky materials were reduced using an 8 mm bar sieve before crushability tests. Then, the entire mass of aggregates (F1–F3) with different size fractions (S1–S3) was fed manually to the jaw crusher (Fig. 4b) in a single charge.

In the crushability tests, nine coupling variables (Fig. 2) were adopted, and five tests were conducted for each coupling variable. In total, 45 crushability tests were performed for each rock type, and average values obtained from the tests were presented.

Throughout the crushing action, the variations in current drawn by the crusher were recorded systematically (Fig. 4c). After the crushability tests, crushed particles were sieved (Fig. 4d) for obtaining quantitative data on their DRCs. For specific size fractions (–9.52 + 6.30 mm and –6.30 + 4.75 mm), flakiness index tests were also carried out (Fig. 4e).

Typical PSDs and current measurements are given in Fig. 5. As a result of crushability tests, the quantitative DRC parameters (i.e., SRR, Δw, FI_{p1-2}, and E_t) were calculated for each case. All these parameters were recorded and transformed into a dataset for further analyses.

The crushability test results are presented in Table 4. From S1–F1 to S3–F3 conditions, the SRR varied from 1.46 to 2.44. The E_t and E_{cs} were found to be between 11.59 and 43.69 kJ and 21.18 – 33.63 kJ/kg, respectively. The results in Table 4 show that the DRC is directly associated with the m_f and F_{80}. The underlying reasons for varying DRC parameters are discussed in the following sections.

4. Results and discussion

4.1. Assessment of the DRC based on response surface methodology (RSM)

The crushability tests demonstrated that the m_f and F_{80} have remarkable impacts on the DRC from different perspectives. To determine dominating factors affecting the DRC parameters, the response surface methodology (RSM) was adopted. The RSM is a useful technique for developing, improving, and optimizing processes or products [38]. It provides absolute values of standardized effects based on Pareto charts. Consequently, the method reveals dominating factors and interactions on dependent variables [39].

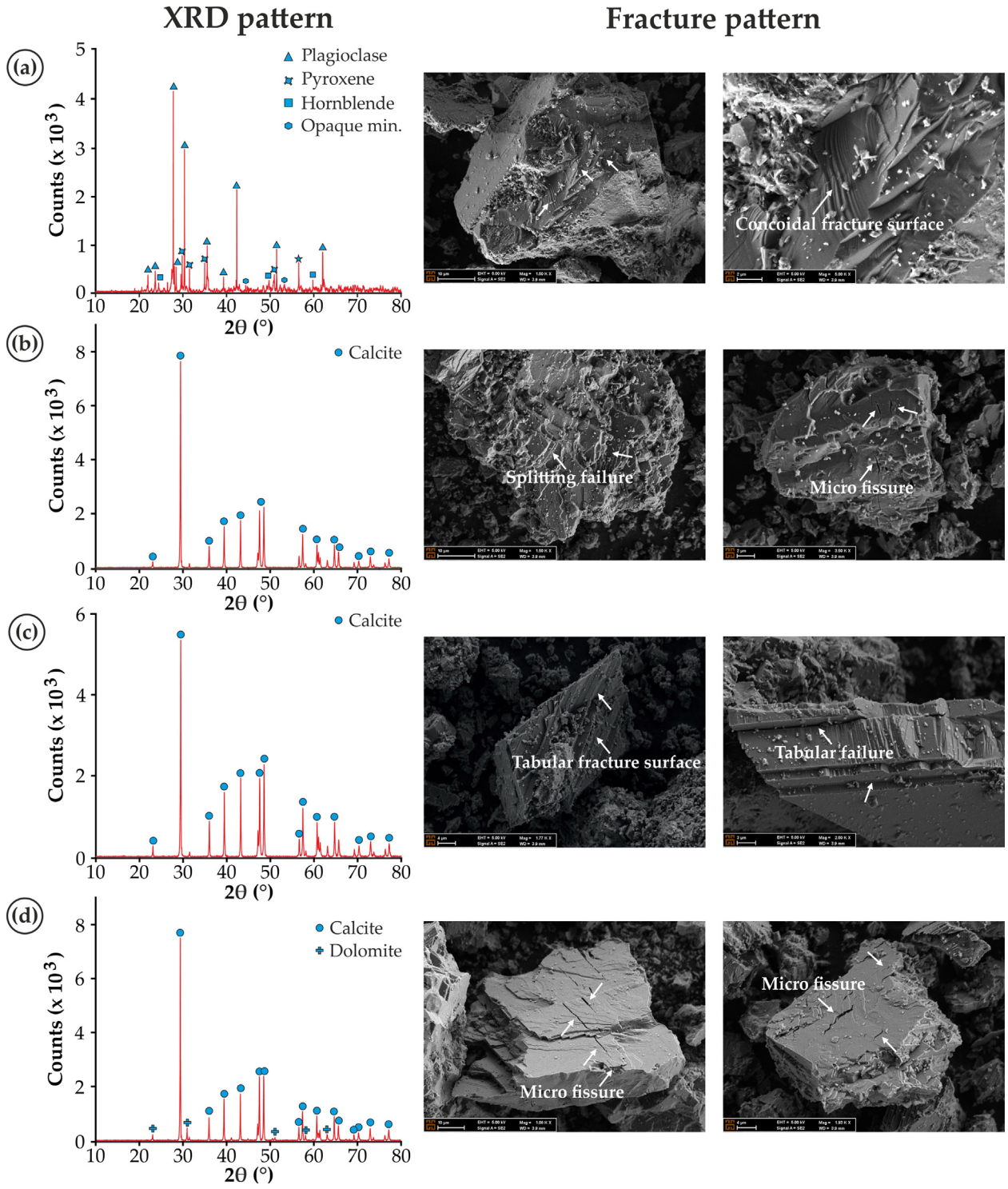

Fig. 3. Typical XRD and fracture patterns of the investigated rocks a) R1 b) R2 c) R3 d) R4.

Table 3
Physicomechanical and aggregate properties of the investigated rocks.

Rock type	Location	Code	γ_n (g/cm^3)	w_a (%)	UCS (MPa)	LAA (%)
Basalt	Çaycuma – Zonguldak	R1	26.10	0.49	113.56	22.29
Limestone	Havran – Balıkesir	R2	25.41	0.30	82.32	21.80
Limestone	Gölbaşı – Ankara	R3	25.62	0.85	64.57	29.72
Dolomitic limestone	Yahyalı – Kayseri	R4	26.29	0.18	120.54	19.61

γ_n : Dry unit weight w_a: Water absorption UCS: Uniaxial compressive strength.
LAA: Los Angeles abrasion value.

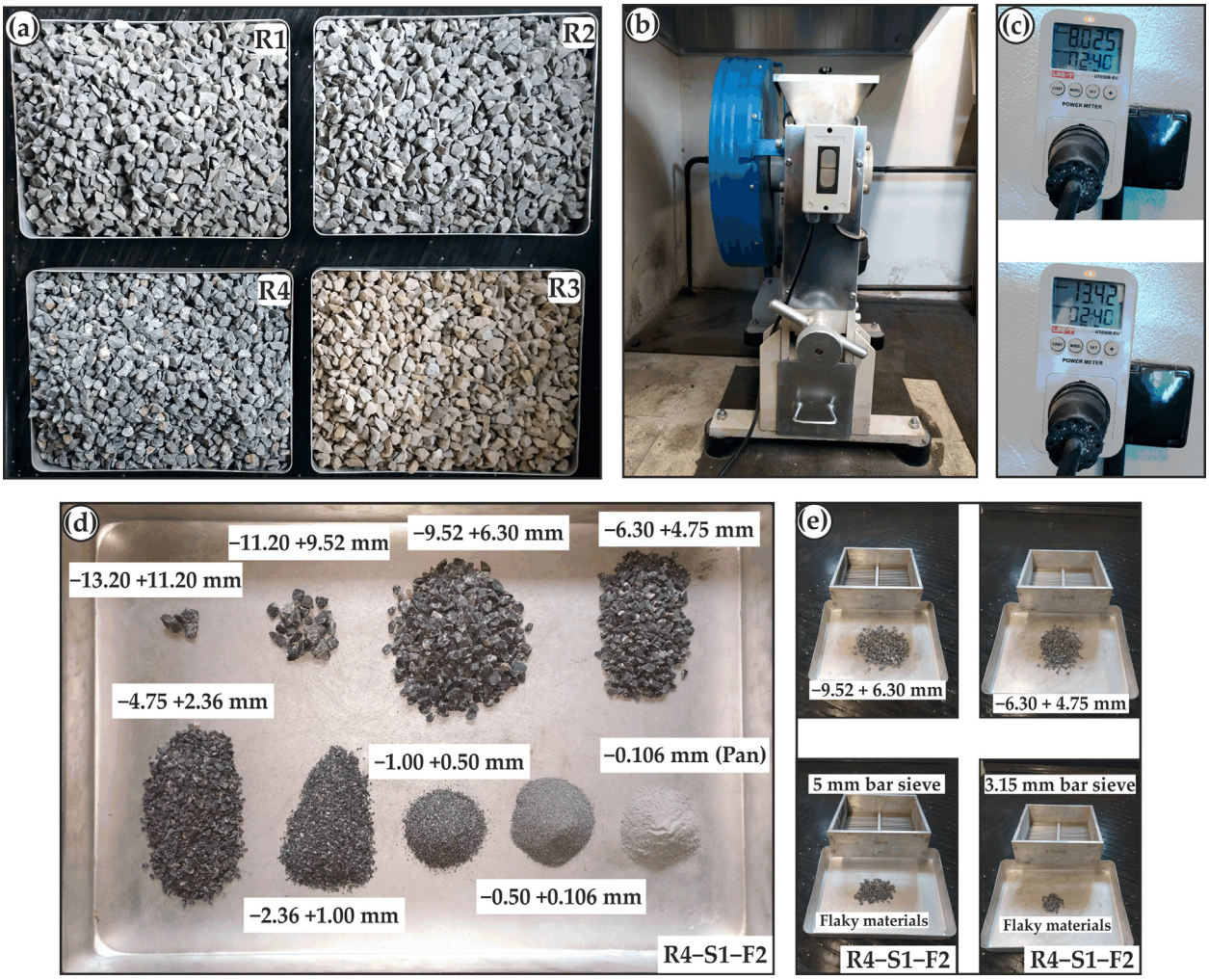

Fig. 4. Rock samples and devices used in the crushability tests a) Rock aggregates with reduced flaky materials (9.52 – 19 mm) b) Laboratory-scale jaw crusher c) Current measurements at different stages of a single crushability test d) Crushed particles after a crushability test e) Flakiness index test for different size fractions.

In this regard, the RSM analyses were conducted through the software Minitab. The linear relationship with interactions (e.g., x_1, x_2, and x_1x_2) was adopted as the fitting function. The feeding properties (Fig. 2), rock properties (Table 3), and all quantitative DRC parameters (Table 4) were integrated into the RSM analyses. The analysis results are given in Fig. 6.

Focusing on the SRR of rocks, the F_{80} dominates the size reduction. Although the Δw is regarded as a size-related parameter, the rock properties (UCS and w_a) and the m_f have more significant effects than the F_{80}. The Δw covers size parameters (Eq (5)) highly dependent upon choke feeding intensity in the crushing chamber. Under this circumstance, rock properties and the m_f became prominent and agreed with Kahraman et al. [26].

Concerning the FI_{p1} and FI_{p2} values, the UCS, w_a, m_f, and F_{80} can together take part in their variations. However, these variables do not act at the same level when considering their standardized effects in Fig. 6. Achieving a lower correlation of determination ($R^2 = 0.57$) for FI_{p1} may be derived from the measurement method. Since there is no standardized bar sieve corresponding to the particle size range of 9.52–6.3 mm, two bar sieves (4 mm and 5 mm) were used together that may cause problems in determining the relevant parameter. Besides, for the determination of FI_{p2}, (6.30–4.75 mm), the 3.15 mm bar sieve conforms to the BS 933–3 [34].

Herein mentioned that the FI_p decreases gradually from S1–F1 to S3–F3 conditions. For R1–R3, the FI_p increases with the decrease in product size. For the same comparison, in contrast, it decreases when considering R4 (Table 4). In either case, further studies are required on whether the product flakiness would be affected by the product's size fractions. Finally, it is evident that the m_f plays a vital role in the E_t (Fig. 6). As a result of the RSM analyses, the m_f and F_{80} can be declared indispensable parts in evaluating the DRC in jaw crushing. Several surface response models are also given in Fig. 6 to evaluate the DRC parameters in more detail.

Basically, in the case of energy concerns, the m_f should be regarded, whereas the F_{80} is essential in general size reduction. The Pareto charts and response surface models reveal the characteristics of the DRC parameters. Although these charts clarify well-dominating factors, they do not state which parameter increases or decreases the response. In these cases, surface response models provide practical information on how effective the factors would be.

For industrial jaw crushers, the choke feeding intensity is not considered a critical phenomenon in initial rock breakage. However, the choke feeding intensity is highly dependent upon the m_f in the crushing chamber. The more the m_f in the crushing chamber, the more fine particles will be produced owing to intense choke feeding activity [4]. As an indirect jaw crushing parameter, the choke feeding intensity was also emphasized by Beloglazov and Ikonnikov [40]. As the rock comminution and energy efficiency can be defined as a function of area increment of particles in jaw

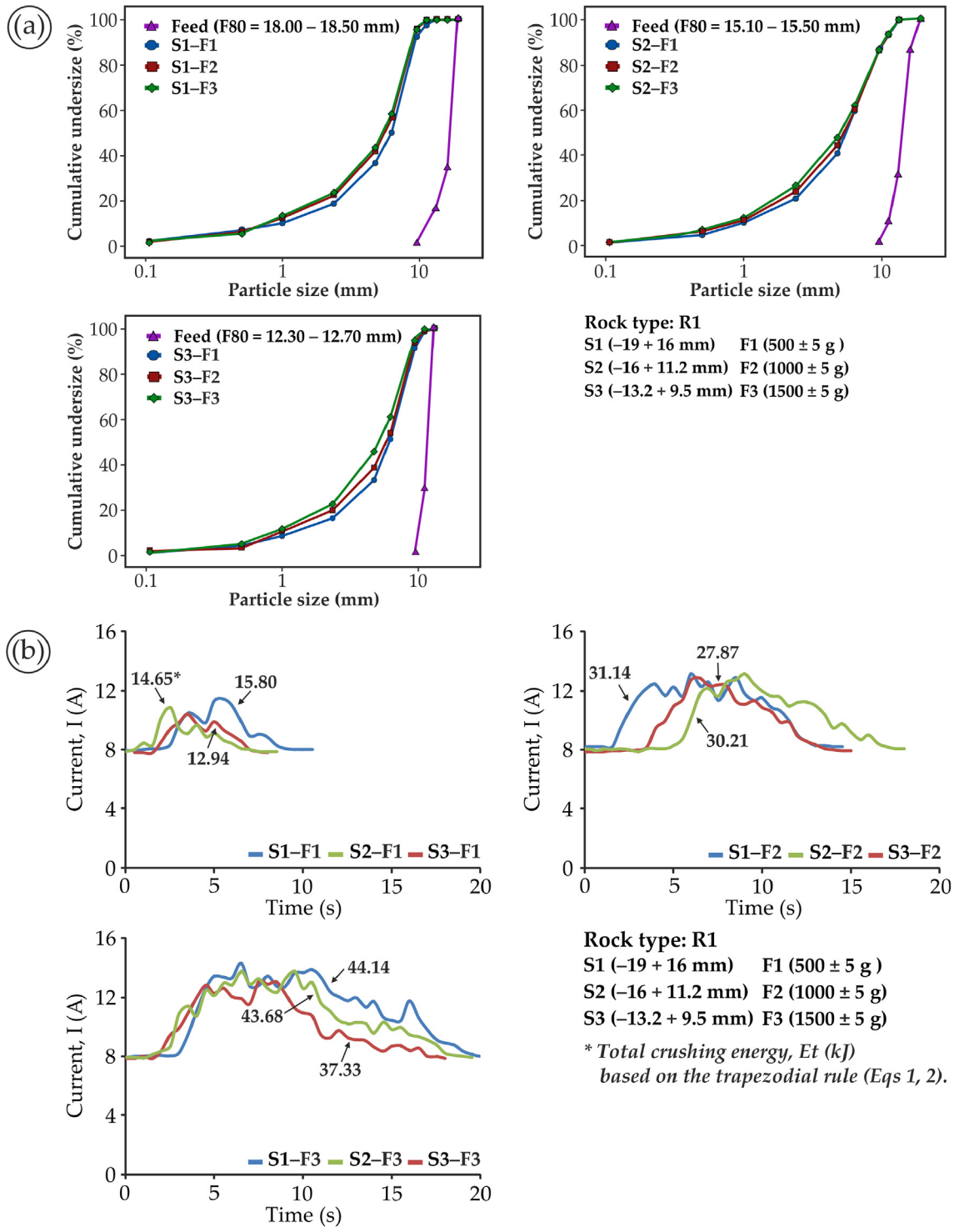

Fig. 5. Effects feeding properties on crushability tests a) PSD of products b) Variations in current drawn by the crusher.

crusher [41], the production of fines can be diminished by regulating the m_f in the crushing chamber. From this point of view, feed level sensors or circuit breaker plugs may be beneficial for the regulation of m_f during jaw crushing. In this way, the crushing energy consumption and the generation of fines can be optimized using these tools.

In order to avoid misconception, it should be mentioned that the crushed particles obtained from both jaw or cone crushers may not be the actual final products ready to be used in such applications. More profoundly, as a global approach, the final shape of products is mainly achieved by reshaping them through a vertical shaft impact crusher [7]. Briggs and Evertsson [42] stated that efficient rock comminution and obtaining optimal shape properties might not be available simultaneously. In some cases, desirable size reduction is accomplished, whereas concerns regarding product shape are met in other cases. Owing to this reason, the

Table 4
Crushability test results.

Rock type	Parameter	S1–F1	S1–F2	S1–F3	S2–F1	S2–F2	S2–F3	S3–F1	S3–F2	S3–F3
R1	SRR	2.14	2.26	2.25	1.83	1.92	1.99	1.46	1.52	1.61
	Δw	0.98	1.10	1.11	0.92	1.00	1.09	0.96	1.06	1.13
	FI_{p1}	18.13	13.82	12.93	13.00	12.30	11.44	8.43	11.69	10.23
	FI_{p2}	26.66	19.90	16.12	17.01	13.97	13.36	15.04	14.06	11.29
	E_t (kJ)	15.38	30.73	44.15	14.66	30.33	43.69	12.94	27.91	37.32
	E_{cs} (kJ/kg)	30.63	30.87	29.37	29.14	30.28	29.09	25.91	27.89	24.91
R2	SRR	2.33	2.39	2.44	1.83	1.85	1.89	1.59	1.65	1.67
	Δw	1.19	1.25	1.28	1.15	1.22	1.29	1.05	1.25	1.25
	FI_{p1}	14.57	10.12	10.86	11.17	11.55	11.90	13.09	13.59	11.02
	FI_{p2}	20.68	17.22	16.72	16.61	15.46	13.84	15.68	14.74	12.59
	E_t (kJ)	12.84	23.67	37.08	12.74	24.35	36.95	13.06	26.70	34.56
	E_{cs} (kJ/kg)	25.45	23.60	24.70	25.56	24.24	24.62	26.04	26.70	23.01
R3	SRR	2.32	2.44	2.44	1.93	1.97	2.05	1.62	1.60	1.70
	Δw	1.24	1.36	1.38	1.21	1.26	1.29	1.12	1.21	1.24
	FI_{p1}	15.69	14.77	14.65	13.20	9.52	10.02	11.78	10.64	11.50
	FI_{p2}	25.06	19.70	22.25	20.40	15.26	18.29	18.70	14.81	15.06
	E_t (kJ)	12.78	22.41	33.38	12.60	21.61	31.81	13.06	21.74	33.06
	E_{cs} (kJ/kg)	25.52	22.33	22.22	25.25	21.54	21.18	26.01	21.74	22.01
R4	SRR	2.25	2.34	2.34	1.89	1.91	1.99	1.56	1.59	1.62
	Δw	1.12	1.16	1.26	1.12	1.16	1.17	1.06	1.13	1.19
	FI_{p1}	21.20	16.07	19.84	23.38	17.80	15.07	17.56	18.90	13.70
	FI_{p2}	14.70	13.60	12.37	12.11	9.20	10.35	8.18	6.94	7.16
	E_t (kJ)	16.88	28.02	42.46	13.43	28.26	42.82	11.59	26.53	41.97
	E_{cs} (kJ/kg)	33.63	28.02	28.28	26.80	28.19	25.53	23.01	26.56	27.95

DRC should be investigated through dynamic simulations or soft computing algorithms, one part of which is introduced in the following section.

4.2. Application of gene expression programming (GEP) for the assessment of DRC

For a detailed evaluation of the DRC, the gene expression programming (GEP) methodology was utilized. The GEP has been used in various science and engineering fields to solve many problems [43–46]. In this regard, a novel application of GEP was presented to predict the DRC parameters. The prediction of DRC parameters provides useful indicators on the performance of crushers.

The GeneXpro software was used in implementing various GEP models. In the models, the number of chromosomes, head sizes, and gen sizes were set to 30, 8, and 3, respectively. The linking function was multiplication, and root means square error (RMSE) was regarded as the fitness function. As a result of the GEP analyses, the empirical formulae of sub-expression trees are given in Table 5.

Apart from the FI_{p1}, the GEP models estimated consistent DRC parameters with a minimum R^2 of 0.76 (Fig. 7). However, the GEP requires a dataset before the calculation can be performed. Owing to this reason, it is not appropriate for crushing design studies. It may instead be useful to analyze the crushing processes by integrating such mathematical models (e.g., Table 5) into Matlab or any other programming languages. In this context, such GEP models may be suitable for optimizing some of the DRC parameters (e.g., E_t) by collecting field data.

Thanks to its dynamic calculations capability, GEP models can also have flexibilities to analyze subsystems of crushing and screening components that can be declared another advantage of GEP.

It was determined that the DRC parameters could be estimated reliably from the GEP models (Fig. 7). The findings obtained from the present study imply that artificial sand–gravel production processes can be optimized by regulating the m_f and F_{80}. However, further studies should also be focused on varying CSS, m_f, and F_{80} combinations. The study clearly shows that the generation of fines will decrease or increase when the m_f and F_{80} are in control. Specific to portable jaw crushers, sand-gravel producers may benefit from this knowledge. The improvements in feed size lead to beneficial optimization in the performance of crushers due to lower system capital costs, reducing unit operating costs, and increasing plant productivity [47]. Also, focusing on the m_f and F_{80} may enable achieving the optimal production yield for specific size fractions, where the GEP can be the right choice of facility in estimating the variations in production yield due to the m_f and F_{80}.

It is worth reminding that excessive fine and flaky materials and lower SRR values are significant evidence of poor rock comminution. It is well-known that the presence of fines deteriorates the rock aggregate quality and decreases the total production yield. In addition, flaky products are not desired in aggregate-related engineering applications or structures since their abrasion resistance is relatively lower than the cubical ones [48,49]. Hence, the crushing operations should be improved, considering crushing-related parameters as many as possible. As such, the number of crushability tests should be increased concerning parametric approaches for a more detailed investigation of DRC.

5. Conclusions

The present study aims to reveal the effects of feeding properties (m_f and F_{80}) on the DRC that occurred in a laboratory-scale jaw crusher. Crushability tests were performed on four rock types, and the variations in DRC parameters were investigated through the RSM. In addition, the DRC parameters were also predicted using the GEP models. The crushability tests provided adequate knowledge of how the rock aggregates behave under the choke feeding domination at different stages.

The RSM analysis results indicated that the m_f and F_{80} are indispensable elements in jaw crushing. The F_{80} controls the general size reduction, whereas the m_f is responsible for the crushing energy consumption and product flakiness. The UCS and w_a are also found to be reasonable parameters for quantifying rock crushability. From S1–F1 to S3–F3 feeding conditions, the FI_p improves slightly. For the same comparison, the E_{cs} decreases gradually, which clearly shows the effects of choke feeding on the DRC. Therefore, it is evident that the choke feeding intensity can be

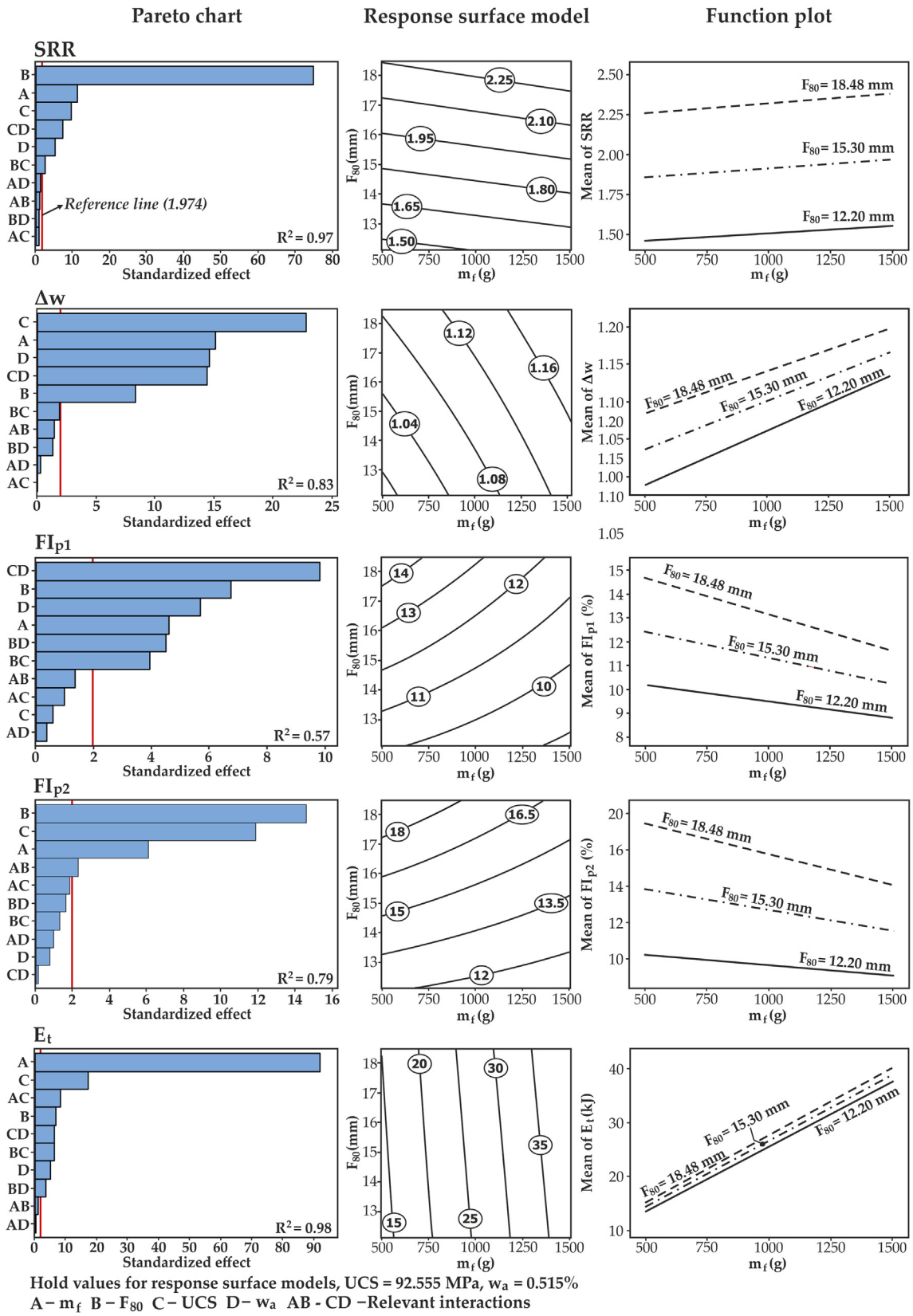

Fig. 6. RSM analysis results.

regulated by changing the m_f and F_{80}. In this way, the generation of fines can be optimized, which may provide a piece of useful information to rock aggregate manufacturers and sand–gravel producers. Several GEP models were also introduced to evaluate the DRC parameters in this study. The proposed GEP models have a satisfactory estimation capability. Therefore, one can claim that

Table 5
Empirical formulae of Sub-ETs for the GEP models.

GEP Model 1 (SRR)	**Sub-ET1**	$(\exp(d_3) + (d_1 + c_1))/2 - d_3$	$g1c_1$ = 5.428
	Sub-ET2	$1/(2d_3 + (c_7 + d_2)/2 + d_0)$	$g2c_7$ = 4.597
	Sub-ET3	$(1/(1 - d_3) + (\ln(c_1) + d_0 + d_1)/2)/2$	$g3c_1$ = 0.285
GEP Model 2 (Δw)	**Sub-ET1**	$\min((((d_1/d_2) + c_9) - (d_3 - c_3)); ((d_1 + c_5)/2 - (d_3 \times c_8)))$	$g1c_9$ = 4.533
	Sub-ET2	$\exp\left(\min(\min(d_3; c_6); (d_3 \times c_7)) - \left((d_3 + c_4)/2 \times c_4^{1/3}\right)\right)$	$g1c_3$ = 122.056
	Sub-ET3	$\max((c_1 \times d_3 \times c_0); (c_2 + d_3)) - ((d_3 + c_8) \times (d_2/d_0))$	$g1c_5$ = 4.550 $g1c_8$ = 4.857 $g2c_6$ = 0.092 $g2c_7$ = 0.307 $g2c_4$ = 3.425 $g3c_0$ = 2.894 $g3c_2$ = 3.844 $g3c_8$ = 3.039 $g3c_1$ = 2.625
GEP Model 3 (FI_{p1})	**Sub-ET1**	$\ln(d_3) + (2(d_1 \times d_2)/(d_0 + c_1) + (d_1 + d_3)/2)$	$g1c_1$ = 1.299
	Sub-ET2	$\max((\max((d_3 + c_6); (c_1/d_3)) - (d_1/c_6)); \ln(d_1 - c_0))$	$g2c_6$ = 4.668
	Sub-ET3	$\left(\left(d_3^2 + 1\right)/d_3 + 1\right)/2 + \ln((c_0 + d_3)/2)$	$g2c_1$ = 2.022 $g3c_0$ = 0.102
GEP Model 4 (FI_{p2})	**Sub-ET1**	$1/(1 - (((d_1 - d_2) + (d_1 - d_2)/d_1)/2))$	$g2c_1$ = 4.645
	Sub-ET2	$\ln(((\max(c_1; c_3) \times (d_3 \times d_1)) \times (d_1 + d_3)) - d_2)$	$g2c_3$ = 4.876
	Sub-ET3	$d_2 - (((d_1 \times c_1) + (d_0 - d_2))/2)/((c_1 - d_0) \times d_3)$	$g3c_1$ = 259.022
GEP Model 5 (E_t)	**Sub-ET1**	$(((d_2/d_0) - c_3) \times c_1) + ((d_1 + d_0) - (c_7/d_3))$	$g1c_1$ = 31.706
	Sub-ET2	$(d_2 - ((c_4 - d_1) + c_0)) - \left((c_3 + d_3) \times c_3^{1/3}\right)$	$g1c_3$ = 5.463
	Sub-ET3	$1/((c_4 \times d_2) - ((d_2 - d_0) - 2c_3))$	$g1c_7$ = 10.601 $g2c_0$ = 4.944 $g2c_3$ = 3.698 $g2c_4$ = 1.887 $g3c_4$ = 18.734 $g3c_3$ = 72.770

d_0: m_f, d_1: F_{80}, d_2: UCS, d_3:w_a.

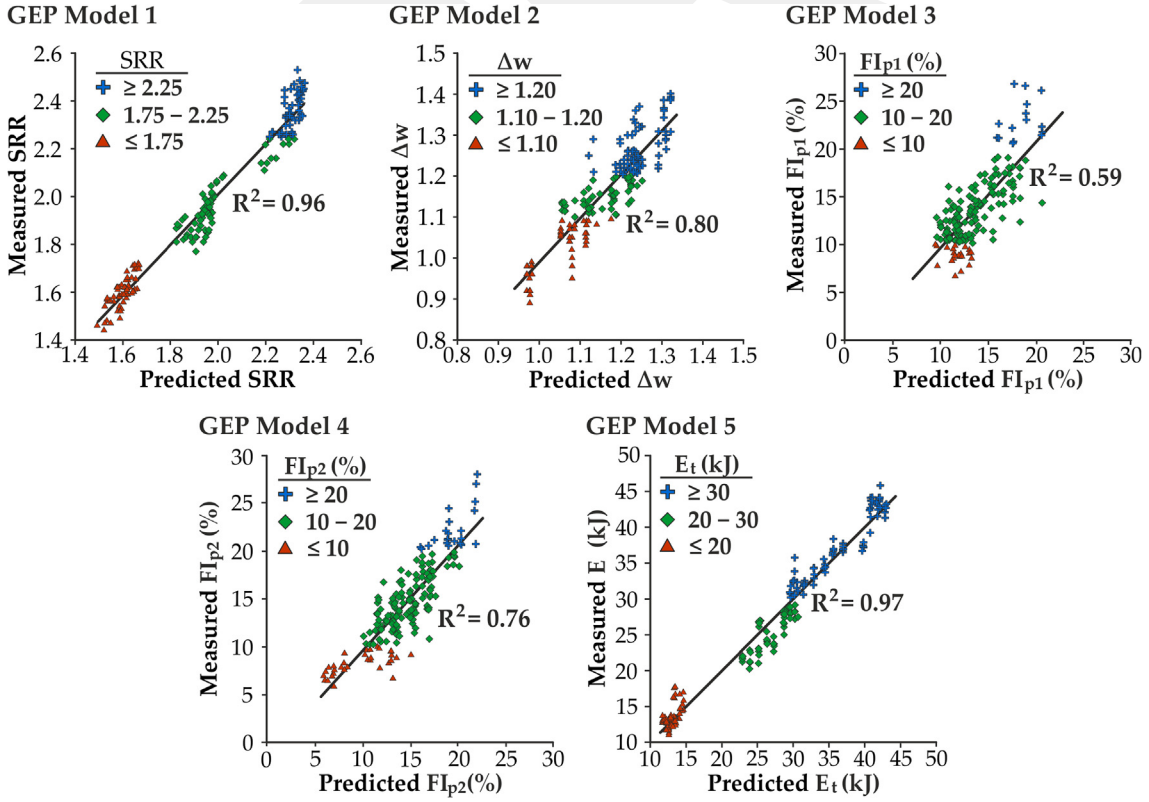

Fig. 7. Correlations between predicted and measured values from the GEP models.

the use of GEP may be a beneficial way for the assessment of issues regarding the optimization of jaw crushing operations. Lastly, the DRC in jaw crushers should be investigated in more detail concerning product achievement. In this context, investigations using a laboratory-scale jaw crusher can represent portable crushing – screening plants endowed with jaw crushers.

Quantitative approaches stated in this study should be attempted in portable crushing – screening plants to observe difficulties/similarities of quantifying such DRC parameters stated in this study. Moreover, the operational features connected with feeding properties should be investigated from technical possibility and commercial concerns. It should be kept in mind that the choke feeding intensity is a critical part of compressive crushers, which varies with physicomechanical and mineralogical features of rocks. Therefore, rock comminution optimizations should be assessed and addressed to individual rock types because the choke feeding intensity has individual impacts on any rock type.

Declaration of Competing Interest

The authors declare that they have no known competing financial interests or personal relationships that could have influenced the work reported in this paper.

Acknowledgments

The authors wish to express their sincere gratitude to anonymous reviewers for their constructive comments and suggestions.

References

[1] J. Donovan, Fracture toughness based models for the prediction of power consumption, product size, and capacity of jaw crushers, Dissertation, Mining and Minerals Engineering Department, Virginia Polytechnic Inst, Blacksburg, 2003.
[2] Duthoit, V. Crushing, and Grinding. Aggregates, Ch. 9, (Ed. Louis Primel and Claude Tourenq). Balkema, Rotterdam, (2000)
[3] R. DeDiemar, New concepts in jaw crusher technology, Miner. Eng. 3 (1–2) (1990) 67–74.
[4] M.S. Guimaraes, J.R. Valdes, A.M. Palomino, J.C. Santamaria, Aggregate production: Fines generation during rock crushing, Int. J. Miner. Process. 81 (2007) 237–247.
[5] M. Bengtsson, P. Svedensten, M. Evertsson, Improving yield and shape in crushing plant, Miner. Eng. 22 (7) (2009) 618–624.
[6] Major, K. Factors influencing the selection and sizing of crushers. In: Malhotra, D. et al., (Eds.), Recent advances in mineral processing plant design. SME, Englewood, USA, (2009), 356–360
[7] Hulthén E. Real-time optimization of cone crushers, Dissertation, Department of product and production development, Chalmers Univ. Tech. Göteborg, (2010).
[8] R. Zolfaghari, M. Karamoozian, Crushing analysis of the industrial cage mill and the laboratory jaw crusher, J. Part. Sci. Tech. 3 (3) (2017) 155–161.
[9] S. Remli, N. Fellouh, T. Batouch, F. Metiri, Optimisation of rock primary crusher yield with the use of scalper, Int. J. Adv. Eng. Man. 4 (2) (2019) 16–20.
[10] Y. Nishida, H. Yoshida, R. Togashi, Introduction of mobile crusher BR580JG-1, Komatsu technical report 53 (2007) 160.
[11] M. Nehring, P.F. Knights, M.S. Kizil, E. Hay, A comparison of strategic mine planning approaches for in-pit crushing and conveying, and truck/shovel systems, Int. J. Min. Sci. Tech. 28 (2018) 205–214.
[12] M. Osanloo, M. Paricheh, In-pit crushing and conveying technology in open-pit mining operations: a literature review and research agenda, Int. J. Min. Rec. Environ. 34 (6) (2019) 430–457.
[13] V.L. Yakolev, V.A. Bersenev, A.V. Glebov, S.S. Kulniyaz, M.A. Marinin, Selecting cyclical-and-continuous process flow diagrams for deep open-pit mines, J. Min. Sci. 55 (5) (2019) 783–788.
[14] Heikkilä P. Improving the quality of crushed rock aggregate, Dissertation, Helsinki Univ. Tech. pp. (1991), 191
[15] Eloranta J. Influence of crushing process variables on the product quality of crushed rock, Dissertation, Tampere University of Technology, (1995)
[16] M. Bengtsson, C.M. Evertsson, An empirical model for predicting flakiness in cone crushing, Int. J. Miner. Process. 79 (1) (2006) 49–60.
[17] M. Johansson, M. Bengtsson, M. Evertsson, E. Hulthén, A fundamental model of an industrial-scale jaw crusher, Miner. Eng. 105 (2017) 69–78.
[18] G.K. Barrios, N. Jimenez-Herrera, F.-T. Natalia, L.M. Tavares, DEM simulation of laboratory-scale jaw crushing of a gold-bearing ore using a particle replacement model, Minerals 10 (2020) 717.
[19] K.A. Abuhasel, A comparative study of regression model and the adaptive neuro-fuzzy conjecture systems for predicting energy consumption for jaw crusher, Applied Sciences 9 (2019) 3916.
[20] M. Fladvad, T. Onnela, Influence of jaw crusher parameters on the quality of primary crushed aggregates, Miner. Eng. 151 (2020) 106338.
[21] Tavares L.M. and Da Silveria M.A.C.W Comparison of measures of rock crushability, In Fine Particle Technology and Characterization, (Meftuni Yekeler Eds), ISBN: 978-81-308-0241-1, (2008)
[22] A. Refahi, J.A. Mohandesi, B. Rezai, Discrete element modeling for predicting breakage behavior and fracture energy of a single particle in a jaw crusher, Int. J. Min. Process. 94 (2010) 83–91.
[23] B.M. Olaleye, Influence of some rock strength properties on jaw crusher performance in granite quarry, Min. Sci. Technol. 20 (2) (2010) 204–208.
[24] Lee E, Evertsson C.M. A comparative study between cone crushers and theoretically optimal crushing sequences. Miner. Eng 24, 188–194.
[25] T. Korman, G. Bedekovic, T. Kujundzic, D. Kuhinek, Impact of physical and mechanical properties of rocks on energy consumption of jaw crusher, Physicochem. Probl. Miner. Process. 51 (2) (2015) 461–475.
[26] S. Kahraman, O.Y. Toraman, S. Cayirli, Predicting the strength and brittleness of rocks from a crushability index, Bull. Eng. Geol. Environ. 77 (4) (2018) 1639–1645.
[27] R. Comakli, S. Cayirli, A correlative study on textural properties and crushability of rocks, Bull. Eng. Geol. Environ. 78 (2019) 3541–3557.
[28] E. Köken, A. Özarslan, New testing methodology for the quantification of rock crushability: Compressive crushing value (CCV), Int. J. Min. Metall. Mater. 25 (2018) 1227–1236.
[29] E. Köken, Evaluation of size reduction process for rock aggregates in cone crusher, Bull. Eng. Geol. Environ. 79 (2020) 4933–4946, https://doi.org/10.1007/s10064-020-01852-5.
[30] E. Köken, Size reduction characterization of underground mine tailings: A case study on sandstones, Nat. Resour. Res. (2020), https://doi.org/10.1007/s11053-020-09707-2.
[31] Legendre D. Numerical and experimental optimization analysis of a jaw crusher and a bubble column reactor, Dissertation, Åbo Akademi University, Turku, (2019)
[32] Itaävuo P., Vilkko M. and Jaatinen A. Indirect particle size distribution control in cone crushers. In 16th IFAC Symposium on automation in mining, mineral and metal processing, 46(16), (2013) 224–229
[33] C.M. Evertsson, Modelling of flow in cone crushers, Miner. Eng. 12 (12) (1999) 1479–1499.
[34] B.S. En, 933–3 British Standards Institution; Tests for geometrical properties of aggregates. Determination of particle shape, Flakiness index (2012).
[35] ISRM. The complete ISRM suggested methods for rock characterization, testing, and monitoring, 1974–2006. In: R. Ulusay, & J. A. Hudson (Eds.), (2007), Suggested methods prepared by the commission on testing methods. International Society of Rock Mechanics (ISRM), Ankara, Turkey
[36] BS EN 1097–2 British Standards Institution; Tests for mechanical and physical properties of aggregates, Methods for the determination of resistance to fragmentation, (2010)
[37] Deere, D. U., & Miller, R. P. Engineering classification and index properties for intact rock. Technical Report Air Force Weapons Laboratory (Report No, AFWL-TR-65-116), (1966), 136–184, New Mexico.
[38] Myers R.H. Response surface methodology : Process and product optimization using designed experiments, 4th ed. (Raymond H. Myers, Douglas C. Montgomery, Christine M. Anderson-Cook. Eds.), Wiley, (2016), ISBN 978-1-118-91601-8
[39] S.M. Kowalski, D.C. Montgomery, Design and analysis of experiments, Minitab manual, 7th edition., Wiley, 2011.
[40] Beloglazov I.I. and Ikonnikov D.A. Computer simulation methods for crushing process in an jaw crusher, In: 2016 IOP Conf. Ser. Mater. Sci. Eng. 142, (2016), 012074
[41] D. Legendre, R. Zevenhoven, Assessing the energy efficiency of a jaw crusher, Energy 74 (2014) 119–130.
[42] C. Briggs, C. Evertsson, Shape potential of rock, Miner. Eng. 11 (2) (1998) 125–132.
[43] H. Çanakcı, A. Baykasoğlu, Güllü H Prediction of compressive and tensile strength of Gaziantep basalts via neural networks and gene expression programming, Neural Comput Appl. 18 (2009) 1031–1041.
[44] D.J. Armaghani, E.T. Mohamad, E. Momeni, Narayanasamy MS An adaptive neuro-fuzzy inference system for predicting unconfined compressive strength and Young's modulus: a study on Main Range granite, Bull. Eng. Geol. Environ. 74 (2015) 1301–1319.
[45] L.P. Leon, D. Gay, Gene expression programming for evaluation of aggregate angularity effects on permanent deformation of asphalt mixtures, Const. Build. Mater. 211 (2019) 470–478.
[46] J. Abdulsalam, A.I. Lawal, R.L. Setsepu, M. Onifade, Bada S Application of gene expression programming, artificial neural network and multilinear regression in predicting hydrochar physicochemical properties, Bioresour Bioprocess 7 (2020) 62.
[47] Napier-Munn, T.J., Morrel J., Morrison R.D. and Kojovic T. Mineral Comminution Circuits: Their Operation and Optimization. Julius Kruttschnitt Mineral Research Centre: Indooroopilly, (1996), ISBN: 9780646288611, 413 pp, Australia
[48] Andersson, E., and Öjerborn, S. Estimation of Rock Quality in Road Projects from Pre-Study to Aggregate (Master thesis), (2014), Chalmers University of Technology, 119 pp, Göteborg.
[49] Benediktsson, S. Effects of Particle Shape on Mechanical Properties of Aggregates (Master thesis), (2015), Norwegian University of Science and Technology, 125 pp, Trondheim.